BMC Cancer

RESEARCH

Open Access

Establishment of CD34 + hematopoietic stem cell-derived xenograft model of hyperleukocytic acute myeloid leukemia

Yanxia Jin[1,2†], Yuxing Liang[1†], Balu Wu[1], Sanyun Wu[1], Xiaoyan Liu[1*] and Fuling Zhou[1,3*]

Abstract

Background Hyperleukocytic acute myeloid leukemia (HLL) is marked by high early mortality and presents significant therapeutic challenges. Research on HLL is still in its infancy, and comprehensive development of patient-derived xenograft (PDX) models, especially CD34 + hematopoietic stem cell-derived models, remains limited.

Methods We evaluated the establishment of the HLL model through blood examinations, smear analysis, bone marrow biopsy, flow cytometry, and mutation analysis. Correlation between survival times in mice and patients was assessed using linear regression.

Results In the HLL PDX mouse model, leukocyte counts could reach up to 37.35^10^9/L, and immunophenotyping revealed the presence of hCD45+, hCD15+, and hCD33 + cells in both peripheral blood (PB) and bone marrow (BM) following inoculation with PB-derived cells for the establishment of the HLL PDX model. Similar results were observed with cells derived from the patient's BM. In the CD34 + hematopoietic stem cell-derived xenograft model, extensive infiltration of CD34 + cells into the BM, liver, and spleen was observed. Additionally, human *WT1* and *NRAS* mutations were identified in the liver, spleen, and BM of the mice. A comparative analysis of multiple experiments revealed that shorter survival times were observed in mice receiving a higher irradiation dose of 2.5 *Gy* and a greater number of cells derived from PB. Additionally, shorter survival times were observed in model mice injected with cells carrying *NRAS*, *DNMT3A*, *FLT3*, or *NPM1* gene mutations. Correlation analysis indicated that the survival times of the mice were significantly associated with the survival status of the patients.

Conclusions We successfully established a CD34 + hematopoietic stem cell-derived xenograft model of HLL, providing a valuable tool for mechanistic research, drug screening, individualized therapy, and precision medicine.

Trial registration Not application.

Keywords Hyperleukocytic acute myeloid leukemia, CD34 + hematopoietic stem cell, Patient-derived xenograft model, B-NSG mice

†Yanxia Jin and Yuxing Liang contributed equally to this work.

*Correspondence:
Xiaoyan Liu
liuxiaoyan@znhospital.cn
Fuling Zhou
zhoufuling@whu.edu.cn

[1]Department of Haematology, Zhongnan Hospital, Wuhan University, Wuhan 430071, Hubei, China
[2]College of Life Sciences, Hubei Normal University, Huangshi 435002, Hubei, China
[3]Research Center for Lifeorgdivision Health, Wuhan University, Wuhan 430071, Hubei, China

Backgrounds

Hyperleukocytic leukemia, a particularly high-risk subtype of leukemia, is typically defined by peripheral blood leukocyte counts exceeding $50–100 \times 10^9$/L [1]. This condition is marked by an abnormal proliferation of white blood cells (WBCs), which significantly increases blood viscosity, leading to complications such as leukocyte stasis [2] and subsequent leukemic infiltration of various organs, including the lungs, liver, and central nervous system. Patients diagnosed with hyperleukocytic acute myeloid leukemia (HLL) often face a grim prognosis, with elevated mortality rates attributed to severe, life-threatening complications [3]. These complications include, but are not limited to, severe respiratory failure [4], disseminated intravascular coagulation (DIC), and tumor lysis syndrome—conditions that collectively exacerbate the already critical nature of the disease [1, 5]. The hyperviscosity and leukostasis can precipitate respiratory and neurological crises, while DIC contributes to widespread clotting and bleeding issues, further complicating patient management.

The early mortality associated with hyperleukocytic leukemia is particularly concerning, with studies indicating that mortality rates can soar as high as 40% within the first week post-diagnosis [6, 7]. This rapid decline underscores the urgency of effective therapeutic interventions. One of the primary treatment strategies is leukapheresis. By mechanically removing excess leukocytes from the bloodstream, leukapheresis not only reduces blood viscosity but also lessens the immediate leukemic cellular burden, offering a critical window of time to initiate definitive treatment [5]. However, while leukapheresis provides rapid relief, it is often used in conjunction with other therapies, such as cytoreductive chemotherapy, to achieve long-term disease control.

To investigate the pathogenesis of HLL and identify effective treatments, establishing a suitable model of HLL is of critical importance. Traditional mouse models of leukemia are often constructed by transplanting immortalized cell lines; however, these cell lines can undergo phenotypic changes that do not accurately reflect the disease's true state [8]. Such alterations may lead to a loss of key disease characteristics, limiting the utility of these models in understanding the complexities of HLL.

The patient-derived xenograft (PDX) model offers a more representative approach by transplanting primary cells from fresh tumor tissues of patients into immunodeficient mice. This model has been widely used to study various cancers, including non-small cell lung cancer, bladder cancer, triple-negative breast cancer [9–11], and acute myeloid leukemia (AML) [12]. The PDX model preserves the original tumor microenvironment and the unique characteristics of the patient's tumor within the mouse, making it a more valuable in vivo tool compared to cell line-based models when studying leukemia [13, 14]. Recent studies have utilized NSGS mice to characterize the engraftment of AML patient samples stratified by risk, revealing important insights into the model's robustness and kinetics [13]. In a study involving 28 AML patient samples, the engraftment was assessed based on molecular and cytogenetic classification. The study demonstrated that, while the majority (85–94%) of mice were successfully engrafted in the bone marrow (BM) regardless of risk group, high-risk (HR) AML cases exhibited significantly superior engraftment levels compared to favorable-risk (FR) and intermediate-risk (IR) cases.

Currently, research on hyperleukocytic acute myeloid leukemia (HLL) is still in its early stages, and the establishment of a patient-derived xenograft (PDX) model for HLL has not been fully reported. Particularly, the development of a CD34 + hematopoietic stem cell-derived xenograft model for HLL remains unexplored. In this study, we address this gap by utilizing NOD.CB17-Prkdc-^{scid}Il2rg^{tm1}/Bcgen (B-NSG) mice, which are characterized by severe immunodeficiency, to establish and evaluate an HLL model [10, 15]. These mice provide a highly suitable platform for the engraftment and study of human HLL cells, given their lack of T cells, B cells, and functional NK cells, which allows for a more accurate representation of human disease and therapeutic responses.

Methods

Patient-derived leukemia cell collection and culture

Human cells were collected from newly diagnosed HLL patients enrolled from Zhongnan Hospital of Wuhan University, and the information for the collected clinical samples is provided in Table 1. Patient diagnosis with AML was based on standard morphological and cytochemical examinations of peripheral blood and marrow smears according to the French-American-British (FAB) and World Health Organization (WHO) criteria.

The HLL cells were collected using a Fresenius COM.TEC machine at Zhongnan Hospital; the procedures were described in our previous reports [16]. Peripheral blood mononuclear cells (PBMCs) were separated with a Ficoll kit according to the manufacturer's instructions (TBD, lot: LDS1075, Tianjin, China). The separated cells were maintained in RPMI 1640 media containing 10% FBS (Gibco, Invitrogen, Carlsbad, CA, USA) with 100 U/ml penicillin and 100 μg/ml streptomycin at 37 °C and 5% CO_2. Bone marrow-derived cells were collected from HLL patients during bone marrow biopsy and separated using a red blood cell lysis buffer.

Isolation of CD34 + cells

CD34 + cells were separated using the CD34 MicoBeads Kit (Miltenyi Biotec, Germany) according to the manufacturer's instructions. In brief, PBMCs from HLL

Table 1 The information of the collected clinical samples

Information		Patient #1	Patient #2	Patient #3
Gender		Male	Male	Female
Age (year)		44	27	28
Clinical diagnosis		AML-M5	AML-M1	AML-M1
Detection of gene mutation (PCR and sequencing)		DNMT3A (+) NRAS (+) NPM1 (+) FLT3-TKD (+)	*WT1* (+) NRAS (+)	*WT1* (+) SET-CAN (+)
Immunophenotype (Flow cytometry)	Abnormal cells ratio	58.50%	74.6%	71.8%
	Immunopheno-type expression	CD36, HLA-DR, CD11b, CD15, CD38, CD33, CD64	CD34, CD33, CD11b, CD7, CD123, CD99, CD71	CD7, CD34, CD33, CD19, CD11b, CD79a, CD38

patients (Patient #2) with WT1 and NRAS mutations were magnetically labeled with CD34 microbeads for 30 min at 4 ℃, and then centrifuged at 300 g for 10 min. The cell suspension was loaded onto a MACS® column with a MACS separator. The magnetically labeled CD34 + cell subpopulations were retained within the column, and the unlabeled cells were washed. After removing the column from the magnetic field, the magnetically retained CD34 + cells were eluted as the positively selected cell fraction.

Animal experiments

Five- to six-week-old female B-NSG mice were obtained from Beijing Biocytogen Co., Ltd. (permission number: SCXK 2016-0004) and maintained in a pathogen-free animal facility in laminar airflow cabinets with a 12 h light/12 h dark schedule. The mice were given free access to an autoclaved rodent diet. All experimental procedures adhered to both institutional and national guidelines for the care and use of laboratory animals. Euthanasia was performed using 3–5% isoflurane (RWD, China) to induce unconsciousness, followed by cervical dislocation to ensure death. All procedures followed the guidelines of the Institutional Animal Care and Use Committee (IACUC) and follows the recommendations of the AVMA (American Veterinary Medical Association) for the euthanasia of laboratory animals.

For HLL PDX model establishment with PBMCs of patients, patient-derived xenografts (PDXs) were constructed as described below. On day 0, B-NSG mice were treated with 0 Gy ($n = 5$) or 2.5 Gy ($n = 5$) χ-rays for total body irradiation and intravenously injected with harvested human HLL cells from Paitient #1 mixed with granulocyte colony-stimulating factor (G-CSF). Every mouse was injected with 1.5×10^7 cells within 24 h of irradiation.

For HLL PDX model establishment with BM-derived cells from patients, PDXs were constructed as described below. On day 0, B-NSG mice were treated with 0 Gy ($n = 5$) or 1.5 Gy ($n = 6$) χ-rays for total body irradiation and intravenously injected with harvested BM-derived cells from a human HLL patient (Patient #3) at day 1. The mice in the 1.5 Gy irradiated group were injected with 2.0×10^6 cells within 24 h of irradiation, and the mice without irradiation were injected with 1.5×10^7 cells. Blood samples were collected at intervals to test whether the model was successfully constructed.

For the $CD34^+$ hematopoietic stem cell-derived xenograft model of HLL, NOD-SCID-IL2rγ^{null} (B-NSG) mice were treated with 1.5 Gy χ-rays for total body irradiation on day 0 and intravenously injected with isolated 1.5×10^7 HLL cells ($n = 5$) or 1.5×10^6 $CD34^+$ cells ($n = 5$) from Patient #2 (WT1 and NRAS mutation) mixed with G-CSF within 24 h of irradiation.

To validate whether these models were successfully constructed, on day 9 peripheral blood was collected through the tail vein in mice. Routine blood tests were performed and body weights were determined at regular intervals. The mice were anesthetized with intraperitoneal (i.p.) injection of sodium pentobarbital administration at 120 mg/kg, then the harvested blood, bone marrow and tissue samples were collected for further analysis. The experimental procedures were approved by Experimental Animal Ethics Committee of Wuhan University.

Routine blood examination

Approximately 50 μL of blood was used for routine blood examination with a Coulter STKS automated blood cell analyzer (Beckman Coulter, USA).

Smear analysis and bone marrow biopsy

Blood smears and bone marrow smears were stained via Wright's staining and observed with a microscope under an oil immersion lens (OLYMPUS BX41) to measure the ratio of leukemia cells.

For the bone marrow biopsy, bone marrow collected from mouse thighs was fixed in formalin and embedded in paraffin for bone marrow examination. The sections were sliced using a slicing machine (Leica RM2016)

and incubated with anti-CD34+ (1:200, BD Biosciences). Finally, the images were observed with an OLYMPUS BX53 microscope.

HE staining and immunohistochemistry

The tissues were fixed with formalin and embedded in paraffin to test the infiltration of leukemic cells by HE staining or immunohistochemistry. For IHC, the tissues were stained with antibodies against human anti-CD45+ (1:200, BD Biosciences) or human anti-$CD34^+$ (1:200, BD Biosciences). The images were observed with an OLYMPUS BX41 microscope.

Flow cytometry

Harvested mouse peripheral blood and bone marrow were treated with RBC lysis buffer, HLL cells from Patient #1 were stained with human anti-CD45-PerCPcy5.5, anti-CD15-FITC, and anti-CD33-PE antibodies (BD Biosciences), and HLL or CD34 + cells from Patient #2 were stained with human anti-CD45-PerCPcy5.5 and anti-CD34-APC antibodies (BD Biosciences). The stained cells were analyzed by flow cytometry (FACS Canto II, FACS Verse, and FACS Diva software, BD Biosciences), and data were analyzed with FlowJo Software.

RNA extraction and quantitative real-time PCR (qPCR) detection

The collected fresh liver and spleen tissues from mice were treated and prepared as single cell suspensions. Then, total RNA from the liver, spleen and bone marrow was extracted with TRIzol reagent (Vazyme, Lot: R401-01). The cDNAs were obtained by Evo M-MLV reverse transcript kits (Accurate Biotechnology Co., Ltd, Lot: AG11705).

All qPCR reactions were performed with the SYBR® Premix Ex Taq™ kit (Takara) for 40 cycles using a fluorescence quantitative PCR instrument (Applied Biosystems ABI 7500). The primer sequences were synthesized by Tsingke Biological Technology (Wuhan, China) and were as follows: (1) human *WT1* gene forward (CAGGCTGC AATAAGAGATATTTTAAGCT) and reverse (GAAGT CACACTGGTATGGTTTCTCA), and (2) human reference gene for *ABL* gene forward (TGGAGATAACACTC TAAGCATAACTAAAGGT) and reverse (GATGTAGTT GCTTGGGACCCA). The positive rate for the WT1 gene in the mice was calculated.

NRAS mutation analysis

DNA was extracted from the liver, spleen and bone marrow using a DNA Extraction System (TIANGEN, Lot: DP304). The PCR primer sequences for the *NRAS* gene were synthesized by Tsingke Biological Technology (Wuhan, China) and were as follows: forward (TAGCT AAGGATGGGGGTTGC) and reverse (ACTGGGCCT CACCTCTATGG). PCR was performed with 2 × Hieff™ PCR Master Mix (YEASEN, Lot: H2001071), and the products were sequenced by Tsingke Biological Technology (Wuhan, China) and analyzed by Chromas software (version 1.62).

Statistical analysis

All statistical comparisons were performed using GraphPad Prism 6.0 software. Survival curves were constructed using SPSS 24.0 software. A *P*-value of < 0.05 was considered statistically significant.

Results

Construction of the HLL model with PBMCs from patients

The individual information of enrolled HLL patients were collected from the electronic patient records and provided in the Table 1. PBMCs were collected from HLL patients who underwent leukapheresis by using a Fresenius COM.TEC blood cell separator. The collected leukocytes were isolated by density gradient centrifugation and cultured. The cell viability of separated leukemic cells was still over 90% after culture for four days (Additional file: Figure S1).

Harvested HLL cells were intravenously injected into B-NSG mice to construct the HLL PDX model, and the integrated workflow strategy is shown in Fig. 1a. The body weights of mice in the 2.5 Gy irradiated group gradually decreased (Fig. 1b). The nonirradiated mice survived longer than the mice in the 2.5 Gy irradiated group, and the survival rate was 66.67% (Fig. 1c). On the 9th day, the immunophenotype ratios of hCD45+, hCD15 + and hCD33 + cells in the 2.5 Gy irradiated group were higher than that of nonirradiated group (Fig. 1d). This shows that the HLL model can be successfully established under these two conditions. Because of the rapid death and poor survival of the mice in the 2.5 Gy irradiated group, we performed related experiments on the nonirradiated group. Routine blood examination showed that WBC counts first increased and gradually decreased in the peripheral blood (PB) of B-NSG mice, and the maximum leukocyte count was above 37.35×10^9/L. The red blood cell counts, platelet counts and hemoglobin content decreased gradually (Fig. 1e-h). Leukemic cells were found on the 9th, 21st and 25th days by blood smear analysis (Fig. 1i), and the immunophenotype ratio of hCD45 + cells increased up to 73.8% gradually in PB (Fig. 1j & Fig. S2). Many leukemic cells infiltrated the bone marrow (BM) on the 25th day and even caused erythrocyte lysis, which was observed on a bone marrow smear (Fig. 1k). The immunophenotype ratio of hCD45 + cells in bone marrow were 43.62% (9.5-75.2%), the hCD15 + cells were 54.07% (3.3-79.9%) and the hCD33 + cells were 48.4% (5.7-80.4%) (Fig. 1l). In addition, the histopathological analysis indicated that a large

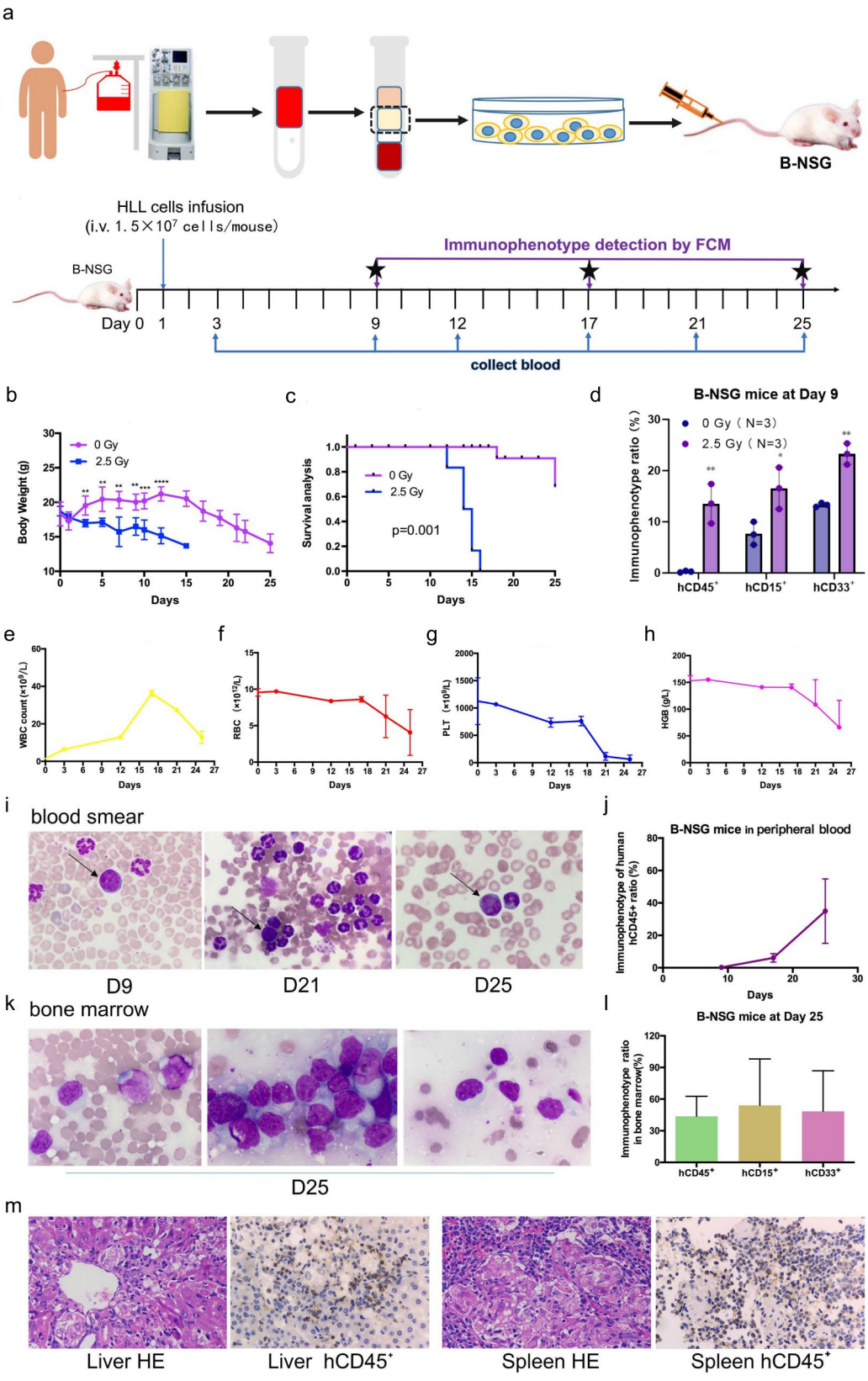

Fig. 1 (See legend on next page.)

(See figure on previous page.)

Fig. 1 Establishment of the model of HLL with PBMCs of patients. (**a**) The HLL cells were collected from HLL patients using a Fresenius COM.TEC machine, and then the PBMCs were separated with a Ficoll kit and cultured. After irradiation at day 0, the B-NSG mice were treated with 0 Gy ($n=5$) or 2.5 Gy ($n=5$) χ-rays for total body irradiation and intravenously injected with harvested from PBMCs of human HLL cells from Patient #1 mixed with granulocyte colony-stimulating factor. Every mouse was injected with 1.5×10^7 cells within 24 h of irradiation at day 1. Blood samples were collected to test the WBC counts at D3, D9, D12, D17, D21 and D25. The immunophenotypes of leukemia cells, including $hCD45^+$, $hCD15^+$ and $hCD33^+$, were detected by flow cytometry on days 9, 7, and 25. (**b**) The body weights were analyzed using GraphPad Prism software (version 8.0) with parametric unpaired t tests. $^{**}P<0.01$, $^{***}P<0.001$, $^{****}P<0.0001$. (**c**) Survival analysis. (**d**) Immunophenotype analysis of leukemia cells. $^{*}P<0.05$, $^{**}P<0.01$. (**e-h**) Routine blood tests with a Coulter STKS automated blood cell analyzer. e, WBC counts. f, RBC counts. g, PLT counts. h, HGB content. (**i**) Blood smear analysis were stained via Wright's staining and observed with a microscope under an oil immersion lens to measure the ratio of leukemia cells. (**j**) Detection of the immunophenotype in peripheral blood by BD FACS Verse flow cytometry. HLL cells were stained with human anti-CD45-PerCPcy5.5, anti-CD15-FITC, and anti-CD33-PE antibodies. (**k**) Bone marrow smear analysis. (**l**) Detection of the immunophenotype in bone marrow by flow cytometry at day 25. (**m**) Histopathological analysis of leukemia cell infiltration into liver and spleen tissues. Magnification: ×400

number of human leukemic cells infiltrated the liver and spleen tissue of the mouse (Fig. 1m).

Construction of the HLL model with BM-derived cells of patients

After experimenting with different irradiation doses, we observed that 2.5 Gy irradiation significantly shortened the survival time of the mice. Therefore, we chose to use a lower dose of 1.5 Gy for bone marrow-derived cells (from Patient #3) to avoid excessive toxicity to the bone marrow microenvironment and improve survival, ensuring a more stable engraftment of hematopoietic stem cells in the B-NSG mice. The body weights were worse and the survival was poorer in the 1.5 Gy group than the 0 Gy group (Fig. 2a, b). Cell morphology analysis showed that human leukemia cells were present in blood smears and detected in blood smear experiments (Fig. 2c, d). Furthermore, the immunophenotype ratios of human leukemia cells in the PB and BM of mice were increased (Fig. 2e, f & Fig. S3, S4).

Successful construction of the CD34 + cell-derived xenograft model

To better explore the HLL model, we constructed a CD34 + hematopoietic stem cell-derived xenograft model of HLL. First, the workflow of model establishment is shown in Fig. 3a. At day 9, the immunophenotypes of hCD45 + and hCD34 + cells were detected at higher ratios in the CD34 + group with PB, and leukemia cells were also detected (Fig. 3b, c), which suggested that the model was successfully established. The body weights of mice in the CD34 + group decreased faster due to the severe tumor load (Fig. 3d). In the CD34 + group, routine blood examination indicated changes, especially the WBC counts and PLT counts (Fig. 3e, f, g, h). On the 25th day, leukemic cells were found by blood smear analysis and flow cytometry (Fig. 3i, j), which were more obviously observed in BM, and the immunophenotype ratios of hCD45 + and hCD34 + cells were slightly increased in the CD34 + group (Fig. 3k, l). Further analysis showed that CD34 + cells infiltrated into the BM, liver and spleen tissues on the 25th day, which indicated more obvious model construction using CD34 + hematopoietic stem cells (Fig. 3m). We also detected gene mutations in mice samples and found that the *WT1* gene was positive in the liver, spleen and BM in mice (Fig. 3n). Moreover, *NRAS* mutations were found in the liver, spleen and BM in mice (Fig. 3o).

Summary of the constructed HLL models with B-NSG mice

The HLL models were constructed for multiple repeated experiments, and the patient information, separated cell characteristics, irradiation doses, injection cell counts, and survival time are summarized in Fig. 4a. By comparison analysis, the mice treated with a higher irradiation dose of 2.5 Gy had a shorter survival time (Fig. 4b), and the more injection of cells derived from PB resulted in a shorter survival time (Fig. 4c). In the absence of irradiation, the constructed model mice injected with cells derived from PB had shorter survival times than the mice injected with cells derived from BM of patients; however, there were no significant differences in survival time between the 1.5 Gy irradiated model mice receiving cells derived from PB and BM (Fig. 4d). Furthermore, mutations of the *NRAS*, *DNMT3A*, *FLT3*, and *NPM1* genes were also analyzed, which indicated that the model mice injected with the *NRAS* gene mutation had a shorter survival time than those injected with cells lacking the *NRAS* gene mutation, and the same results were obtained with the *DNMT3A*, *FLT3*, and *NMPM1* gene mutations (Fig. 4e). In addition, correlation analysis showed that the survival time in mice had a significant correlation with the survival status of enrolled patients (Fig. 4f).

Discussion

In this study, we utilized B-NSG mice, which have a deletion of the interleukin-2 receptor gamma chain (IL2Rγ) and a nearly complete absence of the murine immune system, to construct an HLL model. This choice of model was intended to enhance the engraftment of HLL cells and reduce the incidence of graft-versus-host disease (GVHD) [17, 18]. Our experimental results demonstrated that we successfully established a CD34 + hematopoietic stem cell-derived xenograft model of human HLL in

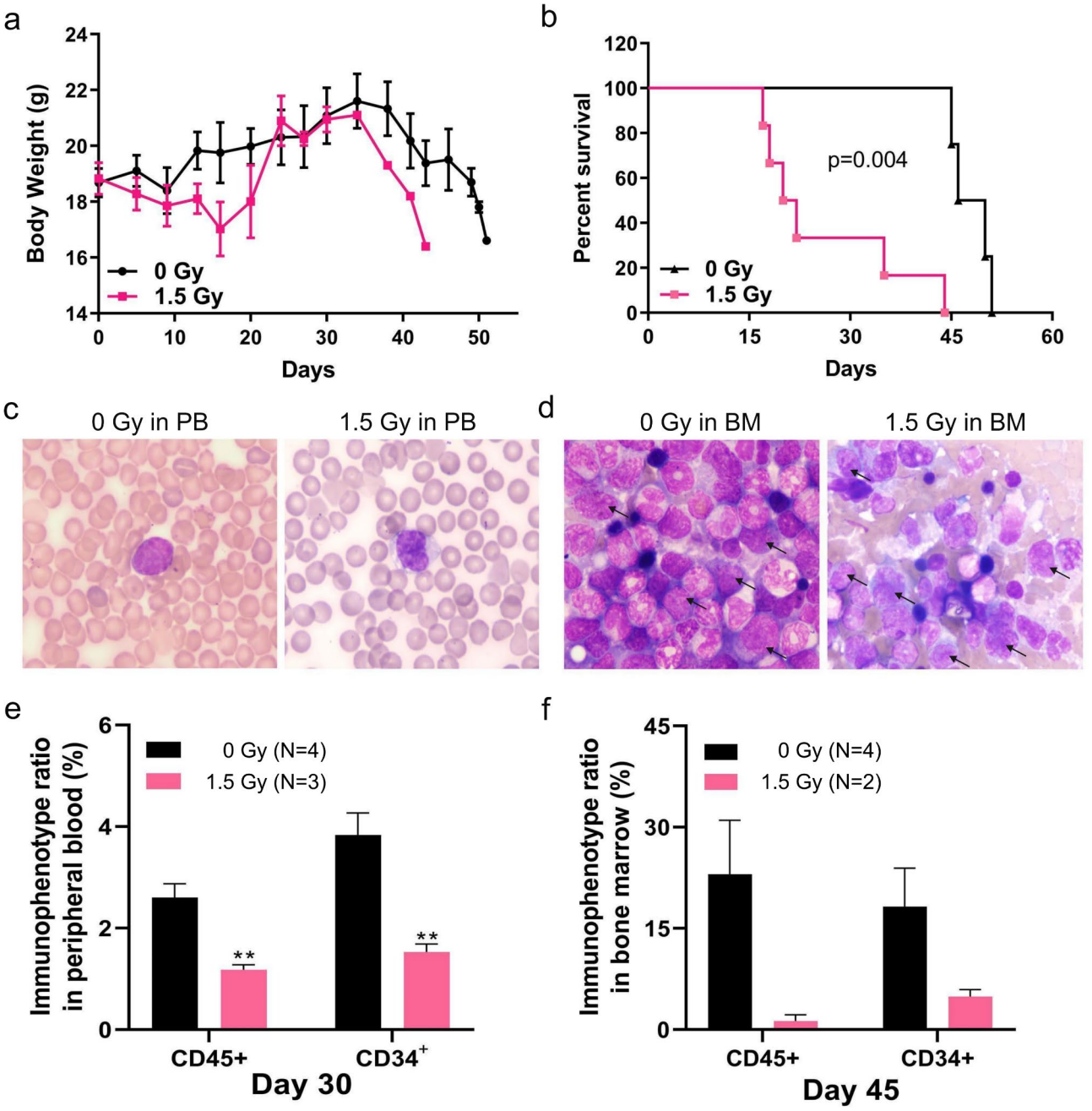

Fig. 2 Construction of the HLL model with BM-derived cells of patients. (**a**) On day 0, B-NSG mice were treated with 0 Gy ($n=5$) or 1.5 Gy ($n=6$) χ-rays for total body irradiation and intravenously injected with harvested BM-derived cells from a human HLL patient (Patient #3) at day 1, then tested the change in body weight at intervals. (**b**) Survival analysis. (**c**) Blood smear analysis. PB, peripheral blood. (**d**) Bone marrow smear analysis. BM, bone marrow. (**e**) Immunophenotype analysis of leukemia cells in peripheral blood at day 30 by flow cytometry. $^{**}P<0.01$. (**f**) Detection of the immunophenotype in bone marrow by flow cytometry after mice were sacrificed

B-NSG mice. Initially, a significant number of HLL cells were detectable in the peripheral blood following the transplantation of cells into the mice, with leukemic cells being clearly observed based on cell morphology in both the peripheral blood and bone marrow. Subsequently, flow cytometry analysis revealed a high ratio of leukemic cell immunophenotypes in the mice, which closely matched those of the patients from whom the cells were derived. Lastly, we observed extensive infiltration of leukemic cells into various tissues, and gene mutations characteristic of the original HLL cells were detected in these infiltrated tissues within the CD34 + hematopoietic stem cell-derived xenograft model.

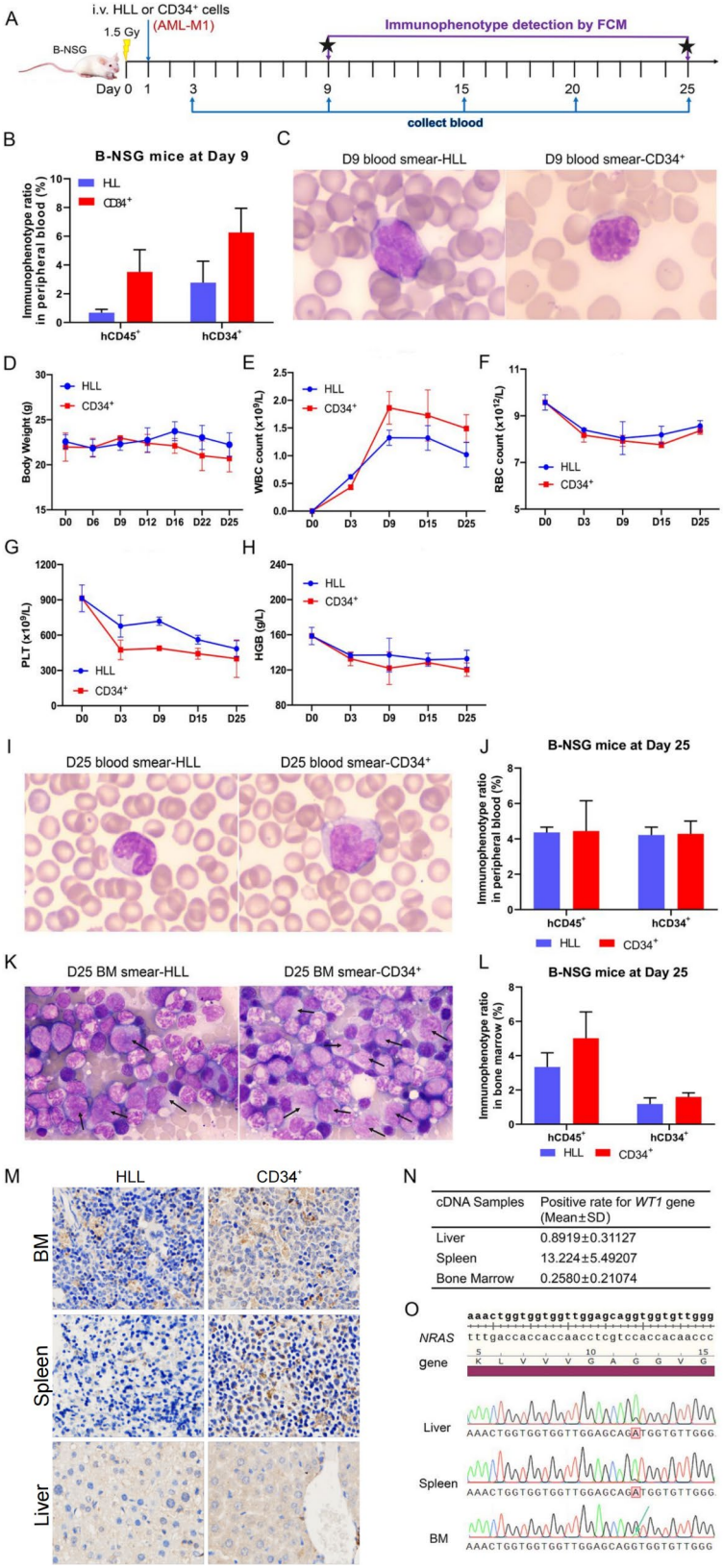

Fig. 3 (See legend on next page.)

(See figure on previous page.)

Fig. 3 Construction of a CD34$^+$ hematopoietic stem cell-derived xenograft model of HLL. (**a**) The workflow of model construction. The B-NSG mice were treated with 1.5 Gy χ-rays for total body irradiation on day 0 and intravenously injected with isolated control cells ($n=5$) or 1.5×10^6 CD34$^+$ cells using magnetic beads ($n=5$) from Patient #2 (WT1 and NRAS mutation) mixed with G-CSF within 24 h of irradiation. (**b**) Detection of immunophenotype in peripheral blood by flow cytometry at day 9. (**c**) Blood smear analysis at day 9. (**d**) The analysis of body weight. (**e-h**) Routine blood tests. e, WBC. f, RBC. g, PLT. h, HGB. (**i**) Blood smear analysis at day 25. (**j**) Detection of immunophenotype in peripheral blood at day 25. The cells were stained with human anti-CD45-PerCPcy5.5 and anti-CD34-APC antibodies. (**k**) Bone marrow smear analysis at day 25. (**l**) Detection of immunophenotype in bone marrow at day 25. (**m**) Immunohistochemical analysis of leukemia cell infiltration into bone marrow, liver and spleen tissues. The tissues were stained with antibodies against human anti-CD45$^+$. BM, bone marrow. (**n**) Detection of the positivity rate of the *WT1* gene using a fluorescence quantitative PCR instrument in tissues of mice in the CD34$^+$ group. (**o**) Detection of *NRAS* mutation in tissues of mice in the CD34$^+$ group. Green represents base A, red represents base T, blue represents base C and black represents base G. The green arrow represents a mutation in BM. BM, bone marrow

According to previous reports, 1.5–3.5 Gy doses of χ-ray radiation have been used before leukemia cell [19–21] or CD34$^+$ cells [22, 23] transplantation into mice, though a few studies have successfully established models without irradiation [24]. For instance, Shafat et al. reported the successful construction of a primary AML model using nonirradiated NSG mice [25]. In this study, we investigated the impact of different radiation doses on the construction of our HLL model. Our findings indicated that mice subjected to 2.5 Gy χ-ray irradiation experienced faster body weight loss and had a shorter survival time compared to those in the nonirradiated (0 Gy) group. This suggests that nonirradiated mice may be more suitable for drug research, as they maintained better overall health and stable body conditions. In contrast, mice in the 2.5 Gy group exhibited poor health, with a median survival time of approximately 17 days, making them less favorable for studying drug efficacy or the mechanisms of HLL development. Irradiation is known to cause transient yet severe myelosuppression [26], which complicates the clear observation of leukemic cells in blood and bone marrow smears, thereby challenging the successful assessment of the model's establishment. Moreover, myelosuppression severely affects routine blood tests, preventing a true evaluation of white blood cell (WBC) dynamics [27, 28]. Our results further demonstrated that irradiation-induced myelosuppression could significantly impact the survival time of the mice, potentially leading to no discernible difference in survival between the 1.5 Gy irradiated models injected with cells derived from peripheral blood (PB) and bone marrow (BM).

In our previous studies on drug screening using a PDX model of HLL, we observed varying survival times for B-NSG mice under different irradiation conditions. Specifically, in the 2.5 Gy irradiated group, B-NSG mice injected with HLL cells that lacked malignant gene mutations survived for more than 20 days [29]. In contrast, nonirradiated B-NSG mice injected with human AML cells isolated from a hyperleukocytic AML-M5 patient harboring *NPM1* and *DNMT3A* mutations survived for over 31 days [30]. Additionally, B-NSG mice subjected to 1.5 Gy irradiation and injected with AML cells from a hyperleukocytic AML-M5 patient with *WT1*, *DNMT3A*, and *FLT3* mutations survived for more than 20 days [31, 32]. The mutational status of AML cells is a critical factor in the construction of a PDX model using immunodeficient mice [33, 34]. In this study, we observed that B-NSG mice injected with AML cells harboring NRAS mutations had shorter survival times compared to those injected with cells lacking *NRAS* mutations. Similar trends were noted for *DNMT3A*, *FLT3*, and *NMPM1* mutations. Importantly, the survival time of the mice was significantly correlated with the survival status of the corresponding patients. These findings suggest that the successful construction of an HLL PDX model using B-NSG mice is strongly influenced by the presence of malignant gene mutations in the HLL cells, which are associated with poor prognosis. Furthermore, the outcome is also dependent on the number of cells injected and the irradiation dosage administered to the mice.

In this study, we successfully established the CD34 + cell-derived PDX model of HLL by treating B-NSG mice with 1.5 Gy χ-ray irradiation and injecting them with CD34 + cells derived from an HLL patient harboring *WT1* and *NRAS* mutations—two mutations frequently associated with AML [35]. These results suggest that B-NSG mice subjected to low-dose radiation are more suitable for model construction when using cells with moderate malignant mutations. However, the HLL model still presents certain limitations. For instance, HLL cells from patients often face challenges in proliferating in vitro, and the mice do not exhibit the full spectrum of clinical characteristics, such as specific immunophenotypes. As a result, the PDX model of HLL remains unstandardized and requires further refinement. Additionally, we have yet to replicate the complex immune microenvironment in immunodeficient mice [36], which limits our ability to fully explore the intricate heterogeneity of HLL and the interactions between HLL cells and their microenvironment [14, 37]. Despite these challenges, further experiments will be conducted to address these issues. Nonetheless, the HLL mouse model remains a valuable tool for studying the pathogenesis of the disease and evaluating drug efficacy.

A

List the experiments for establishment of HLL model with B-NSG mice

Patient-derived cells types	Patient survival	Survival months of patient	Patient cells-derived	Gene mutation types with patient cells	Number of mice	X-ray irradition at D0	Injection of cell counts	Survival times when sacrifice	Published/unpublished
AML-M5	death	15	PB	No mutation	19	2.5 Gy	1.7×10^7/mouse HLL cells	20 days	J Exp Clin Cancer Res, 2018. 37(1): 277
AML-M5	death	10	PB	NPM1, DNMT3A	11	0 Gy	1.5×10^7/mouse HLL cells	31 days	Carbohydr Polym, 2020. 240: 116329.
AML-M5	death	20	PB	WT1, DNMT3A, FLT3	16	1.5 Gy	1.0×10^7/mouse HLL cells	21 days	Oxid Med Cell Longev, 2020. 2020, 1295984.
AML-M5	death	20	PB	WT1, DNMT3A, FLT3	23	2.0 Gy	2.0×10^7/mouse HLL cells	20 days	Free radical bio med, 2019. 146: 275-286.
AML-M5	death	10	PB	NRAS, NPM1, DNMT3A	5	2.5 Gy	1.5×10^7/mouse HLL cells	17 days	Unpublished
AML-M5	death	10	PB	NRAS, NPM1, DNMT3A	5	0 Gy	1.5×10^7/mouse HLL cells	25 days	Unpublished
AML-M1	death	17	PB	WT1, NRAS	5	1.5 Gy	1.5×10^7/mouse HLL cells	25 days	Unpublished
AML-M1	death	17	PB	WT1, NRAS	5	1.5 Gy	1.5×10^6/mouse CD34+ cells	25 days	Unpublished
AML-M1	live	2	BM	WT1	6	1.5 Gy	2×10^6/mouse CD34+ cells	44 days	Unpublished
AML-M1	live	2	BM	WT1	5	0 Gy	1.5×10^7/mouse HLL cells	51 days	Unpublished
AML-M5	death	20	PB	WT1, DNMT3A, FLT3	28	1.5 Gy	1.0×10^7/mouse HLL cells	31 days	Unpublished

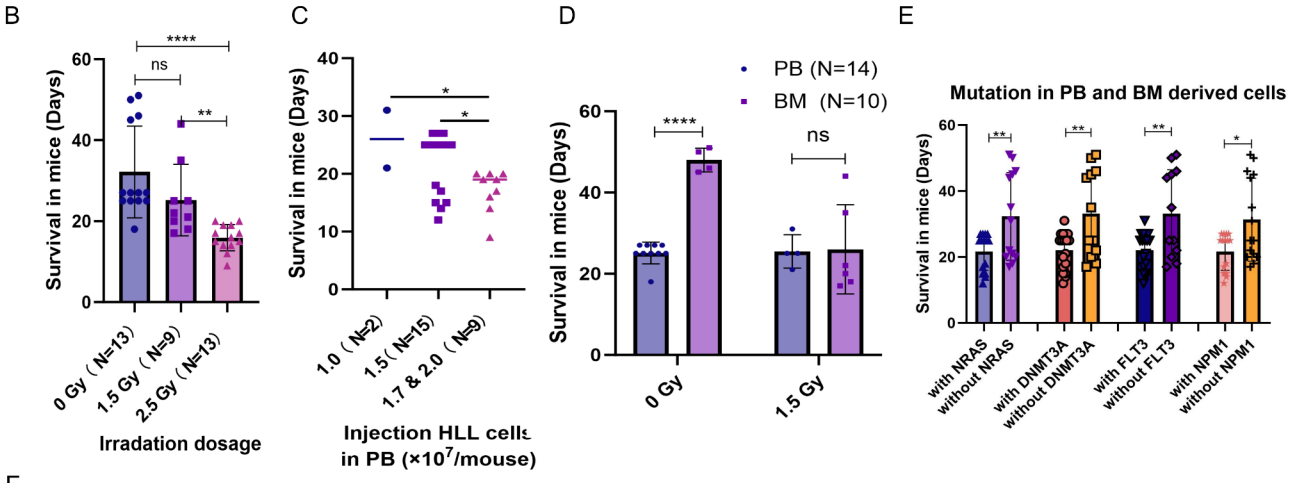

F

The correlation analysis between the survival time in mice and in patients

Item	Unstandardized B	95% CI for B	Standardized Coefficient Beta	t	p value	r^2
Survival time in mice	-0.456	-0.809~-0.104	-0.726	-2.987	0.017	0.527

Fig. 4 Summary of HLL models constructed with B-NSG mice. (**a**) List of experiments for HLL model establishment in B-NSG mice intravenously injected (i.v.) with patient-derived cells at D1. PB, peripheral blood. BM, bone marrow. The survival months were calculated from leukapheresis to presentation as of March 2021. (**b**) Analysis of the survival time in mice at different irradiation dosages. (**c**) Analysis of the survival time in mice with different injection cell counts from the PB of patients. (**d**) Analysis of the survival time in mice injected with cells derived from PB and BM with irradiation of 0–1.5 Gy. (**e**) Analysis of survival time in mice with different gene mutations. (**f**) Correlation analysis was performed to characterize the correlation between the survival time in mice and in patients by a linear regression model with variable selection "entered" with SPSS software (version 26.0). $^{*}P<0.05$, $^{**}P<0.01$, $^{****}P<0.0001$. ns, no significance

Conclusion

In conclusion, we successfully transplanted hyperleukocytic leukemia cells into severely immunodeficient B-NSG mice, which preserved most of the original characteristics of the disease and more accurately simulated tumor growth as observed in clinical patients. We thoroughly assessed and optimized the methods for constructing the HLL model, leading to the successful establishment of a CD34 + hematopoietic stem cell-derived xenograft model of HLL in B-NSG mice. This model provides a valuable tool for mechanistic research, drug screening, individualized therapy, clinical efficacy assessment, and precision medicine in HLL.

Abbreviations

HLL	Hyperleukocytic acute myeloid leukemia
PDX	Patient derived xenograft
WBCs	White blood cells
AML	Acute myeloid leukemia
PB	Peripheral blood
BM	Bone marrow

Supplementary Information

The online version contains supplementary material available at https://doi.org/10.1186/s12885-025-13907-5.

Supplementary Material 1

Acknowledgements
Not applicable.

Author contributions
FZ and YJ conceived the study and provided the project direction. YJ and YL designed, executed and performed the experiments, analyzed the data and wrote the manuscript until the final submission version. BW, SW, and XL helped to collect the patients' information, separate the cells from patients, executed and interpreted the animal experiments. YL performed the MTT assays. BW carried out the qPCR and assisted and supervised the smear analysis. SW assisted and supervised the flow cytometry. FZ and XL revised the manuscript. All authors read and approved the final manuscript.

Funding
This article was supported by the Natural Science Foundation of China (NSFC) programme (No. 82370176) and Hubei Province key research and development plan (No. CZKYXM2023036JZ).

Data availability
All data are available in the main text or the Supplementary materials. Individual participant data underlying the results presented in this article—including text, tables, figures, and appendices—will be available to researcher proposal. Requests for access should be sent to zhoufuling@whu.edu.cn. Data requestors must agree to sign a data access agreement before access is granted.

Declarations

Ethics approval and consent to participate
The study was carried out followed the Declaration of Helsinki and approved by the Research Ethics Committee of Zhongnan Hospital at Wuhan University (license number: 2017048). Informed written consent was obtained from the HLL patients.

Consent for publication
Not applicable.

Competing interests
The authors declare no competing interests.

Received: 31 August 2024 / Accepted: 11 March 2025
Published online: 18 March 2025

References

1. Bertoli S, Picard M, Berard E, Griessinger E, Larrue C, Mouchel PL, et al. Dexamethasone in hyperleukocytic acute myeloid leukemia. Haematologica. 2018;103(6):988–98.
2. Giammarco S, Chiusolo P, Piccirillo N, Di Giovanni A, Metafuni E, Laurenti L, et al. Hyperleukocytosis and leukostasis: management of a medical emergency. Expert Rev Hematol. 2017;10(2):147–54.
3. Feng S, Zhou L, Zhang X, Tang B, Zhu X, Liu H, et al. Impact Of ELN Risk Stratification, Induction Chemotherapy Regimens And Hematopoietic Stem Cell Transplantation On Outcomes In Hyperleukocytic Acute Myeloid Leukemia With Initial White Blood Cell Count More Than 100 x 10(9)/L. Cancer Manag Res. 2019;11:9495–503.
4. Bretz CA, Savage SR, Capozzi ME, Suarez S, Penn JS. NFAT isoforms play distinct roles in TNFalpha-induced retinal leukostasis. Sci Rep. 2015;5:14963.
5. Rollig C, Ehninger G. How I treat hyperleukocytosis in acute myeloid leukemia. Blood. 2015;125(21):3246–52.
6. Ali AM, Mirrakhimov AE, Abboud CN, Cashen AF. Leukostasis in adult acute hyperleukocytic leukemia: a clinician's digest. Hematol Oncol. 2016;34(2):69–78.
7. Stefanski M, Jamis-Dow C, Bayerl M, Desai RJ, Claxton DF, Van de Louw A. Chest radiographic and CT findings in hyperleukocytic acute myeloid leukemia: A retrospective cohort study of 73 patients. Med (Baltim). 2016;95(44):e5285.
8. Pan C, Kumar C, Bohl S, Klingmueller U, Mann M. Comparative proteomic phenotyping of cell lines and primary cells to assess preservation of cell type-specific functions. Mol Cell Proteom. 2009;8(3):443–50.
9. Chaturvedi A, Herbst L, Pusch S, Klett L, Goparaju R, Stichel D, et al. Pan-mutant-IDH1 inhibitor BAY1436032 is highly effective against human IDH1 mutant acute myeloid leukemia in vivo. Leukemia. 2017;31(10):2020–8.
10. Okada S, Vaeteewoottacharn K, Kariya R. Application of highly immunocompromised mice for the establishment of Patient-Derived xenograft (PDX). Models Cells. 2019;8(8).
11. Wang M, Yao LC, Cheng M, Cai D, Martinek J, Pan CX, et al. Humanized mice in studying efficacy and mechanisms of PD-1-targeted cancer immunotherapy. FASEB J. 2018;32(3):1537–49.
12. Griessinger E, Andreeff M. NSG-S mice for acute myeloid leukemia, yes. For myelodysplastic syndrome, no. Haematologica. 2018;103(6):921–3.
13. de la Díaz R, Velasco-Hernandez T, Gutiérrez-Agüera F, et al. Engraftment characterization of risk-stratified AML in NSGS mice. Blood Adv. 2021;5(23):4842–54.
14. Almosailleakh M, Schwaller J. Murine models of acute myeloid leukaemia. Int J Mol Sci. 2019;20(2).
15. Maletzki C, Bock S, Fruh P, Macius K, Witt A, Prall F, et al. NSG mice as hosts for oncological precision medicine. Lab Invest. 2020;100(1):27–37.
16. Jin Y, Guo S, Cui Q, Chen S, Liu X, Wei Y, et al. A hospital based retrospective study of factors influencing therapeutic leukapheresis in patients presenting with hyperleukocytic leukaemia. Sci Rep. 2018;8(1):294.
17. Shultz LD, Lyons BL, Burzenski LM, Gott B, Chen X, Chaleff S, et al. Human lymphoid and myeloid cell development in NOD/LtSz-scid IL2R gamma null mice engrafted with mobilized human Hemopoietic stem cells. J Immunol. 2005;174(10):6477–89.
18. Covassin L, Laning J, Abdi R, Langevin DL, Phillips NE, Shultz LD, et al. Human peripheral blood CD4 T cell-engrafted non-obese diabetic-scid IL2rgamma(null) H2-Ab1 (tm1Gru) Tg (human leucocyte antigen D-related 4) mice: a mouse model of human allogeneic graft-versus-host disease. Clin Exp Immunol. 2011;166(2):269–80.
19. Busfield SJ, Biondo M, Wong M, Ramshaw HS, Lee EM, Ghosh S, et al. Targeting of acute myeloid leukemia in vitro and in vivo with an anti-CD123 mAb engineered for optimal ADCC. Leukemia. 2014;28(11):2213–21.
20. Martelli MF, Di Ianni M, Ruggeri L, Falzetti F, Carotti A, Terenzi A, et al. HLA-haploidentical transplantation with regulatory and conventional T-cell adoptive immunotherapy prevents acute leukemia relapse. Blood. 2014;124(4):638–44.
21. Dong S, Chen J. SUMOylation of sPRDM16 promotes the progression of acute myeloid leukemia. BMC Cancer. 2015;15(1):893.
22. Demmerath E, Bohler S, Kunze M, Erlacher M. In vitro and in vivo evaluation of possible pro-survival activities of PGE2, EGF, TPO and FLT3L on human hematopoiesis. Haematologica. 2019;104(4):669–77.
23. He X, Zhu Y, Lin Y, Li M, Du J, Dong H, et al. PRMT1-mediated FLT3 arginine methylation promotes maintenance of FLT3-ITD + acute myeloid leukemia. Blood. 2019;134(6):548–60.
24. Gopalakrishnapillai A, Kolb EA, Dhanan P, Bojja AS, Mason RW, Corao D, et al. Generation of pediatric leukemia xenograft models in NSG-B2m mice: comparison with NOD/SCID mice. Front Oncol. 2016;6:162.
25. Shafat MS, Oellerich T, Mohr S, Robinson SD, Edwards DR, Marlein CR, et al. Leukemic blasts program bone marrow adipocytes to generate a protumoral microenvironment. Blood. 2017;129(10):1320–32.
26. Lu L, Wang YY, Zhang JL, Li DG, Meng AM. p38 MAPK inhibitor insufficiently attenuates HSC senescence administered Long-Term after 6 Gy total body irradiation in mice. Int J Mol Sci 2016;17(6).
27. Sun C, Yang J, Pan L, Guo N, Li B, Yao J, et al. Improvement of Icaritin on hematopoietic function in cyclophosphamide-induced myelosuppression mice. Immunopharmacol Immunotoxicol. 2018;40(1):25–34.

28. Chisaki Y, Terada T, Yano Y. Population pharmacodynamic model for bayesian prediction of myelosuppression profiles based on routine clinical data after gemcitabine and carboplatin treatment. Pharmacology. 2016;98(5–6):284–93.
29. Jin Y, Yang Q, Liang L, Ding L, Liang Y, Zhang D, et al. Compound Kushen injection suppresses human acute myeloid leukaemia by regulating the Prdxs/ROS/Trx1 signalling pathway. J Exp Clin Cancer Res. 2018;37(1):277.
30. Jin Y, Cai L, Yang Q, Luo Z, Liang L, Liang Y, et al. Anti-leukemia activities of selenium nanoparticles embedded in nanotube consisted of triple-helix beta-d-glucan. Carbohydr Polym. 2020;240:116329.
31. Zhang D, Luo Z, Jin Y, Chen Y, Yang T, Yang Q, et al. Azelaic acid exerts antileukemia effects against acute myeloid leukemia by regulating the Prdxs/ROS signaling pathway. Oxid Med Cell Longev. 2020;2020:1295984.
32. Zhang D, Liu Y, Luo Z, Chen Y, Xu A, Liang Y, et al. The novel thioredoxin reductase inhibitor A-Z2 triggers intrinsic apoptosis and shows efficacy in the treatment of acute myeloid leukemia. Free Radic Biol Med. 2020;146:275–86.
33. Culen M, Kosarova Z, Jeziskova I, Folta A, Chovancova J, Loja T, et al. The influence of mutational status and biological characteristics of acute myeloid leukemia on xenotransplantation outcomes in NOD SCID gamma mice. J Cancer Res Clin Oncol. 2018;144(7):1239–51.
34. Paczulla AM, Dirnhofer S, Konantz M, Medinger M, Salih HR, Rothfelder K, et al. Long-term observation reveals high-frequency engraftment of human acute myeloid leukemia in immunodeficient mice. Haematologica. 2017;102(5):854–64.
35. Kunimoto H, Meydan C, Nazir A, Whitfield J, Shank K, Rapaport F, et al. Cooperative epigenetic remodeling by TET2 loss and NRAS mutation drives myeloid transformation and MEK inhibitor sensitivity. Cancer Cell. 2018;33(1):44–e598.
36. Vago L, Gojo I. Immune escape and immunotherapy of acute myeloid leukemia. J Clin Invest. 2020;130(4):1552–64.
37. Cook GJ, Pardee TS. Animal models of leukemia: any closer to the real thing? Cancer Metastasis Rev. 2013;32(1–2):63–76.

Publisher's note